Properties of a "phase transition" induced by antiangiogenetic therapeutical protocols

M. Scalerandi and F. Peggion

INFM, Dipartimento di Fisica, Politecnico di Torino, Torino, Italy

(Received 15 March 2002; published 19 September 2002)

Inhibiting angiogenesis has been found to be an interesting therapeutical strategy against cancer. In fact, the success of tumor growth is subordinated to the corresponding increase of the vascular system feeding the neoplasm. However, optimization and design of proper antiangiogenetic therapeutical strategies is still an open problem. We apply a recently developed angiogenesis model to study how variations in the relevant parameters, e.g., induced by chemicals, may cause a "phase transition" to a region in the parameter space in which angiogenesis is not succesful. To demonstrate the reliability of our approach and its usefulness, we will study some specific drugs and use our model to investigate the influence of the main variables involved in a clinical treatment: the administration time, the duration of the drug effect, and the drug dose.

I. INTRODUCTION

The concepts of phase transitions, critical parameters, chaotic systems, etc., have found in recent years important applications in medicine and biology. Indeed, in several cases the medical community has taken advantage of intuitions coming from physics for clinical applications, e.g., for the analysis of cellular differentiation [1] or for the understanding of the cardiac rhythm [2].

At the same time, several models for the description of the cell (or of cluster of cells) have been developed starting from the physical and biochemical properties of the cell elements (membrane, mitochondrion, receptors, etc.). Among them, in the last few years models have been formulated to describe the dynamics of tumor growth [3–5] and/or angiogenesis [i.e., the vascular growth induced by the tumor itself through the emission of tumor angiogenetic factors (TAFs)] [6–9].

Most of these models aim to become tools for the development and/or optimization of therapies. To this purpose, from the point of view of a physicist, a drug may be interpreted as an agent acting on a "order parameter" in order to induce a "phase transition" from a region in the parameter space in which the pathology is uncontrolled to a phase in which it is latent, or even regressing [10].

This issue in a biophysical system is more complex than in other physical systems. In fact, from a microscopic point of view, it is required to model many steps and different pathways in which a drug acts chemically on the cell to modify the relevant parameters. Also, the relation between the drug dose and the parameter variation is a nontrivial issue to solve. However, from our point of view, we target the problem at a mesoscopic level, assuming therefore the previously mentioned issues to be someway solved. Nevertheless several problems remain to be faced. First of all, it is essential to discriminate the "order parameters" from the (several) nonrelevant ones. Then, the line separating different phases in the parameter space are to be determined keeping in mind that they may be located differently according to the state of the system, i.e., evolve with time. In fact, at least in pathological cases, biological systems are far from equilibrium. As a consequence, a specific drug may be efficient (i.e.,

inducing the transition) or not, depending on the stage of the pathology at which it is applied.

In the field of oncology, it is well recognized that the existence of a suitable vascular system is a prerequisite for cancer growth [11]. In fact, since the presence of specific molecules is fundamental to induce the proliferation of neoplastic cells, nutrient availability is usually a limiting factor for the development of a tumor [12]. Indeed, cancer cells have a high rate of nutrient consumption (i.e., are biologically strongly aggressive) and tend to exhaust the available nutrient, being its preexisting local sources finite in number (i.e., the number of vessels is limited). The ensuing scarcity of nutrient would force the tumor to remain in a latent stage or enter in remission, unless new capillaries start to grow in the tumor neighborhood, providing a reinforced vascular structure that ensures the feeding of the cancer cells (angiogenesis) [13,14].

As a consequence, inhibiting angiogenesis can be an effective means of controlling cancer development. Several antiangiogenetic treatments are currently under study and even used in clinical trials [15]. These therapies present additional advantages with respect to traditional approaches [16–26]. In fact, endothelial cells (ECs), forming vessel walls and the new capillaries, are genetically more stable than tumor cells, and thus much less capable of acquiring drug resistance [18]. Also, antiangiogenetic drugs are extremely specific, i.e., their action is limited to the newly formed vascular system having very little effects on the host system. However, several problems (such as optimization and efficiency evaluation) have still to be addressed [27].

To help biologists and clinicians solve these issues, recently several models have been developed to predict the evolution of the angiogenetic process [6–9]. In fact, once proven their reliability and accuracy, models may pave a way to determine which are the more relevant parameters affecting the succesful completion of angiogenesis [28]. Furthermore, once it has been well defined on which parameters of the model a specific antiangiogenetic drug acts (and the effect is quantified), simulations can be of great help in the formulation and optimization of therapeutical courses [29].

We have recently developed a model based on the local interaction simulation approach [30]. The essential ingredi-

ent in our approach is the competition between several cell species for nutrient and for TAF [8,9]. In this model, cells are considered as particles with an internal energy, which fore-ordain their behavior and nutrients and TAF distributions evolve according to a "reaction-diffusion equation" with nonstationary sources and sinks [4,31–33]. A preliminary application of the model has led to several results in agreement with biological and clinical observations. In particular, our approach predicts a directional growth from the preexisting vessels towards the tumor front [8], a qualitatively correct morphology and distribution of the capillaries network [9] and the vessels infiltration in the tumor mass [34].

Numerical results have shown that only a few model parameters are relevant for the success of angiogenesis. In fact, we have shown the existence of regions in the parameter space (in particular, for what concerns the remodeling capability and the absorption rate of angiogenetic signals by ECs) in which angiogenesis fails [8]. Also, the survival probability of the new (not yet mature) vessels plays an important role for the completion of the angiogenetic process [34]. Although very preliminary, numerical results are in agreement with clinical data and suggest ways for therapeutical synergy to develop an important point since synergistic interaction of different inhibitors may be crucial for the development of effective anticancer therapies [20,22,25].

However, in previous papers [8] we have not designed real therapeutical strategies, but rather discussed the possible effects of drugs applied and effective during all the angiogenetic process. For a more realistic analysis of the therapeutical effects, the time of administration, the drug dose, and the duration of its effect must be included in the treatment. An analysis of the influence of such parameters have to be understood and may reveal new and interesting effects. An example can be to suggest the optimal approach, chosen according to the stage reached by angiogenesis when the therapy is planned. Analyzing some of these effects of the model, what we have recently proposed is specifically the purpose of this paper.

In the following section, we will recall briefly the main features of our model for angiogenesis. Also, we will mention the basic biological features of some antiangiogenetic drugs and relate them to some of the model parameters. Finally, in Sec. III several examples of applications will be presented and numerical results in general agreement with preliminary clinical observations will be shown.

II. THE MODEL

A. Biophysical model

The basic biophysical model at the two-dimensional level consists of a discretization of the slab of tissue considered in a rectangular grid with space step ε. At each grid point (i,j) and any time t, also discretized with step τ, we define the density of ECs. According to their function, we consider three types of ECs: detached ECs that migrate towards the TAF source $c_{ij}^t(1)$, coalescing ECs that form unstable sprouts $c_{ij}^t(2)$, and ECs that belong to stable blood-transporting vessels $c_{ij}^t(3)$. We also define the nutrient and signal (i.e., TAF) concentrations $n_{ij}^t(1)$ and $n_{ij}^t(2)$, respectively.

Initially, we locate in the lattice some preexisting blood vessels (which are the initial sources of mobile endothelial cells and provide nutrient to the tissue) and a tumor (which is the source of TAF and is assumed to be stationary during the evolution of the system). The problem of the concomitant evolution of the neoplasm and the vascular system has been analyzed elsewhere [34].

The system is described by a "reaction-diffusion equation" model with nonstationary sinks and sources. It is built upon the following few biological and physical assumptions.

(a) Cells are particles with an internal energy $b_{ij}^t(l)$ (where $l=1,2,3$ is the species index) resulting from the balance between nutrient absorption (feeding), consumption (to perform metabolic functions), and release (outflow of molecules from the cell internal part through membrane transporters). The behavior of the cell (mitosis, apoptosis, or quiescence) is completely foreordained by the time changes in the amount of internal energy.

(b) The metabolic state of the cell, and consequently its consumption, may be modulated by signals. In particular, TAFs reduce the normal ECs metabolism, redirecting energy consumption to provide more energy for duplication. In this sense, TAFs behave as growth factors.

(c) TAF diffuses in the region surrounding the tumor and signals ECs to move and reproduce.

(d) Mobile ECs $c(1)$ can coalesce in tubes and sprouts forming temporary structures $c(2)$.

(e) Once the local EC concentration is sufficiently high, the structures stabilize and become blood transporting $c(3)$. Vessel connectivity must be ensured, i.e.,, the transformation $c(2) \rightarrow c(3)$ is allowed only when there are preexisting $c(3)$ cells in the immediate neighborhood.

(f) TAF generation is inhibited once the total nutrient reaching the tumor surpasses a certain threshold.

B. Mathematical implementation

The biophysical model, described in the preceding section, is implemented as a set of nonlinear coupled iteration equations. We will report them in the following section.

1. Equations for nutrients and signals

Nutrients are molecules provided to the tissues from blood-transporting vessels, which behave as localized sources $S_{ij}^t(1)$ with magnitude proportional to the local vessel surface area, hence proportional to the number of $c_{ij}^t(3)$. Effects of TAFs on vessels permeability (the proportionality constant) are neglected here.

The nutrient concentration $n_{ij}^t(1)$ evolves according to

$$n_{i,j}^{t+\tau}(1) = n_{ij}^t(1) + \alpha_p \sum_{nn} [n_{nn}^t(1) - n_{ij}^t(1)]$$

$$+ S_{ij}^t(1) - \Xi_{ij}^t(1) - \Psi, \tag{1}$$

where the sum is performed over the nearest neighbors (nn),

α_p is the nutrient diffusion coefficient, $\Xi(1)$ is the nutrient uptake by ECs (its expression is given later), and Ψ is a constant representing the sink due to the uptake by nonendothelial cells.

A similar ''reaction-diffusion equation'' holds for TAFs generated by tumor cells:

$$n_{ij}^{t+\tau}(2)=n_{ij}^{t}(2)-\varkappa_v n_{ij}^{t}(2)$$

$$+\alpha_v\sum_n [n_{nn}^{t}(2)-n_{ij}^{t}(2)]+S_{ij}^{t}(2)-\Xi_{ij}^{t}(2),$$

$$(2)$$

where α_v is the TAF diffusion coefficient, $S_{ij}^{t}(2)$ is the TAF source term localized on the tumor surface, and $\varkappa_v$ takes into account the unbound TAF degradation rate. TAF absorption by endothelial cells $\Xi(2)$ is introduced below.

2. Equations for ECs

From a physical point of view, all EC species behave as particles with internal energy $b_{ij}^{t}(l)$, which is updated according to an energy conservation law between absorbed $\gamma_{ij}^{t}(l)$, consumed $\beta_{ij}^{t}(l)$, and released $kb_{ij}^{t}(l)$ energy:

$$b_{ij}^{t+\tau}(l)=b_{ij}^{t}(l)+\gamma_{ij}^{t}(l)-\beta_{ij}^{t}(l)-kb_{ij}^{t}(l). \quad (3)$$

It results that

$$\Xi_{ij}^{t}(1)=\sum_{l=1}^{3} [\gamma_{ij}^{t}(l)-kb_{ij}^{t}(l)]. \quad (4)$$

The energy absorbed by an EC belonging to the lth population is $\gamma_{ij}^{t}(l)=A_{ij}^{t}\Gamma_l$, where Γ_l is the maximum possible energy uptake by a single cell during each time step (proportional to the number of receptors), and

$$A_{ij}^{t}=1-\exp\left[\frac{-\Phi n_{ij}^{t}(1)}{\sum_l \Gamma_l c_{ij}^{t}(l)}\right] \quad (5)$$

gives an absorption proportional to the amount of available nutrient, when $n_{ij}^{t}(1)$ is small, and saturates to 1 when the nutrient available is large. This process describes a partial receptor inactivation when nutrient is scarce. Φ is a normalization coefficient that mimic the fact that molecules diffusive processes are faster than other processes involved in the problem.

Energy is consumed partly to perform basic metabolic functions (and this portion is constant with time) and partly to perform additional functions, which may be inhibited by the presence of TAFs:

$$\beta_{ij}^{t}(l)=\beta_0(l)+\bar{\beta}_{ij}^{t}(l). \quad (6)$$

Equations for $\bar{\beta}_{ij}^{t}(l)$ are given later.

A cells's fate is determined by the availability of energy. Defining the energy scale so that the apoptosis threshold corresponds to $b_{ij}^{t}(l)=0$, three situations can occur.

(i) Apoptosis, if $b_{ij}^{t}(l)<0$. The number of eliminated cells increases with the nutrient defect according to a Michaelis-Menten distribution.

(ii) Quiescence, if $0\leq b_{ij}^{t}(l)\leq M$ (M is a mitosis threshold parameter). Cells perform their normal metabolic functions. Note also that ECs not belonging to permanent structures have intrinsic finite lifetimes. The corresponding death rates will be denoted by $\mathrm{s}(l)$:

$$c_{ij}^{t+\tau}(l)=c_{ij}^{t}(l)-\mathrm{s}(l)c_{ij}^{t}(l).$$

(iii) Mitosis, if $b_{ij}^{t}(l)>M$. Cells duplicate and the daughter cells belong to the $c(1)$ population. Duplication occurs at a rate Ω and there is an amount W of energy consumed to perform duplication. The remaining internal energy is equally redistributed among parents and daughter cells. For the $l=1$ population, we have

$$c_{ij}^{t+\tau}(1)=c_{ij}^{t}(1)+\Omega c_{ij}^{t}(1),$$

$$b_{ij}^{t+\tau}(1)=\frac{b_{ij}^{t}(1)(1-W)}{(1+\Omega)}.$$

Similar equations hold for the other populations.

3. Equations for the cell-TAF interaction

In the absence of TAFs, $\bar{\beta}_{ij}^{t}(l)$ is constant. However, the arrival of TAFs signals a modification in the cell metabolic functions:

$$\bar{\beta}_{ij}^{t}(l)=\beta_1(l)\exp[-\chi_l G_{ij}^{t}(l)], \quad (7)$$

where the parameters $\beta_1(l)$ and χ_l characterize the strength of TAF influence on cell metabolism. The quantity

$$G_{ij}^{t}(l)=\xi_l\left[1-\exp\left(-\frac{n_{ij}^{t}(2)}{\sum_l c_{ij}^{t}(l)\xi_l}\right)\right] \quad (8)$$

represents the rate of TAF absorption by each cell belonging to the lth species. Note the similarity between Eqs. (8) and (5), being ξ_l proportional to the number of TAF receptors for the lth species (the equivalent of the number of nutrient receptors Γ_l). As a consequence, ξ_l may be considered as a TAF absorption rate (at least for low values of TAF concentrations). The concentration of extracellular TAF must be correspondingly reduced: $\Xi_{ij}^{t}(2)=\Sigma_l G_{ij}^{t}(l)c(l)$.

4. Equations for cell transformations

ECs evolve from one species to another

$$c_{ij}^{t}(l+1)\rightarrow c_{ij}^{t}(l+1)+\lambda_l c_{ij}^{t}(l)\Theta[c_{ij}^{t}(l)-Q_l], \quad l=1,2,$$

$$c_{ij}^{t}(l)\rightarrow(1-\lambda_l\Theta[c_{ij}^{t}(l)-Q_l])c_{ij}^{t}(l), \quad (9)$$

where λ_l is the transformation rate and Q_l is the transformation threshold. The latter is assumed to be zero for the trans-

formation $1 \rightarrow 2$, since also isolated ECs have been observed to form tubular structures [13].

In addition, we recall that $c(1)$ cells diffuse in the specimen with the usual discretized linear diffusion equation [30]

$$c_{ij}^{t+\tau}(1) = c_{ij}^t(1) + \alpha_c \sum_{nn} [c_{nn}^t(1) - c_{ij}^t(1)],$$

where nn denotes the nearest neighbors of the node i,j and α_c is the cell diffusion coefficient.

C. Antiangiogenetic therapies

As already mentioned, several antiangiogenetic therapies are already used in clinical trials [13]. However, if only their macroscopic effect is considered, such drugs may be grouped into three classes:

(1) Type I: drugs that interfere with angiogenic ligands. An instance could be the monoclonal antibody $2C3$ [26] and the PTK787/ZK 222584 [17], both inhibit the vascular endothelial growth factor (VEGF) receptor 2.

(2) Type II: drugs that modify (either upregulate the production or directly deliver) the distribution of endogenous inhibitors, such as the metalloproteinase inhibitor BB-94 [25] (metalloproteinase is an essential ingredient for remodeling).

(3) Type III: drugs that target directly the vascular system, such as angiostatin [25] or endostatin [23], which inhibits proliferation or induce apoptosis, respectively.

As mentioned in the Introduction, we model the drug action at a mesoscopic level, i.e., by varying some of the model parameters, assuming the relation between the drug dose and the parameters relative change is known. Relevant to describe the effects of the therapy are some quantities related to the therapeutical protocol adopted: the times of administration of the drug (T_n, where $n=1,\ldots,N$, being N the number of treatments), the durations of the therapeutical effect (D_n), and the drug effect on the involved parameter (E_n expressed as a percent variation with respect to the original value).

As already analyzed in Refs. [8,9], the success of the angiogenetic process strongly depends on the values of some relevant model parameters, in particular the VEGF absorption rate $\xi = \xi_1 = \xi_2 = \xi_3$, i.e., the number of active TAF receptors (assumed to be the same for the three ECs species) and the tubes-to-vessels threshold Q_2, i.e., the remodeling capability. In Fig. 1, we show the region in the parameter plane (ξ, Q_2) where we predict successful angiogenesis. Similar curves (see Fig. 4(b) in Ref. [9]) are a characteristic of our model for any set chosen for the other model parameters. Figure 1 shows that there is a sharp separation among a successful phase (located under the curve) and a region in which angiogenesis fails.

The figure suggests that therapeutical strategies may be described as features that, taken a system with parameters lying in the successful angiogenesis region (e.g., point A), move it to the unsuccessful angiogenesis phase.

In particular, in this paper we will discuss the action of the following therapies, which in principles may be all success-
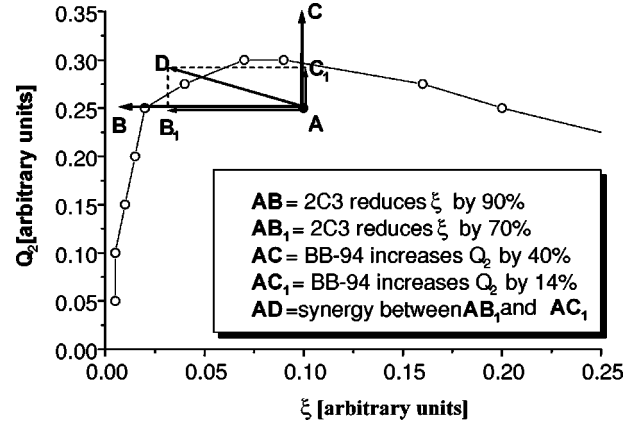
FIG. 1. Phase diagram in the TAF absorption coefficient—remodeling threshold space. The region below the curve corresponds to the one in which angiogenesis is successful. Therapies act on the model parameters in order for the system to cross the separation line between the two phases, as depicted in the figure for a few selected examples.

ful if applied at sufficiently early stages of angiogenesis:

Therapy I. The monoclonal antibody $2C3$ inhibits the VEGF receptor 2 [26], i.e., reduces ξ and moves the system to the point B. The TAF absorption parameter is then defined as

$$\xi(t) = \begin{cases} (1-E_n)\xi, & T_n < t < T_n + D_n, \quad n=1,\ldots,N \\ \xi & \text{otherwise.} \end{cases}$$

We choose $E_n = 0.9$.

Therapy II. The metalloproteinase inhibitor BB-94 [25] reduces the remodeling capability of ECs, hence increases Q_2: the system is moved to the point C. We choose $E_n = -0.4$.

Therapy III. A combined action of the two previous therapies. We apply an increase in Q_2 of 14% (A-$C1$) and a reduction in ξ of 70% (A-$B1$). The two therapies applied separately are supposed not to have an effect strong enough to inhibit angiogenesis. The two acts linearly on the parameters, so the combined therapy (A-D) is expected to be successful. However, we will also show that the effects of the two therapies will not combine linearly (albeit, as remarked, they act linearly on the parameters), but rather an efficient synergic action develops.

In addition, we consider (therapy IV) the application of endostatin, which has the effect of increasing the intrinsic death rate of the newly formed vessels [23], hence by introducing a natural apoptosis rate R_{ang}:

$$c(l) \rightarrow c(l)(1 - R_{ang})\Theta(c(3) - Q_{ang}), \quad l=1\ldots 3. \tag{10}$$

The threshold Q_{ang} is introduced to keep into account that this process holds only for the newly formed vessels, i.e., as long as the density of $c(3)$ is not large enough to guarantee their full maturation.
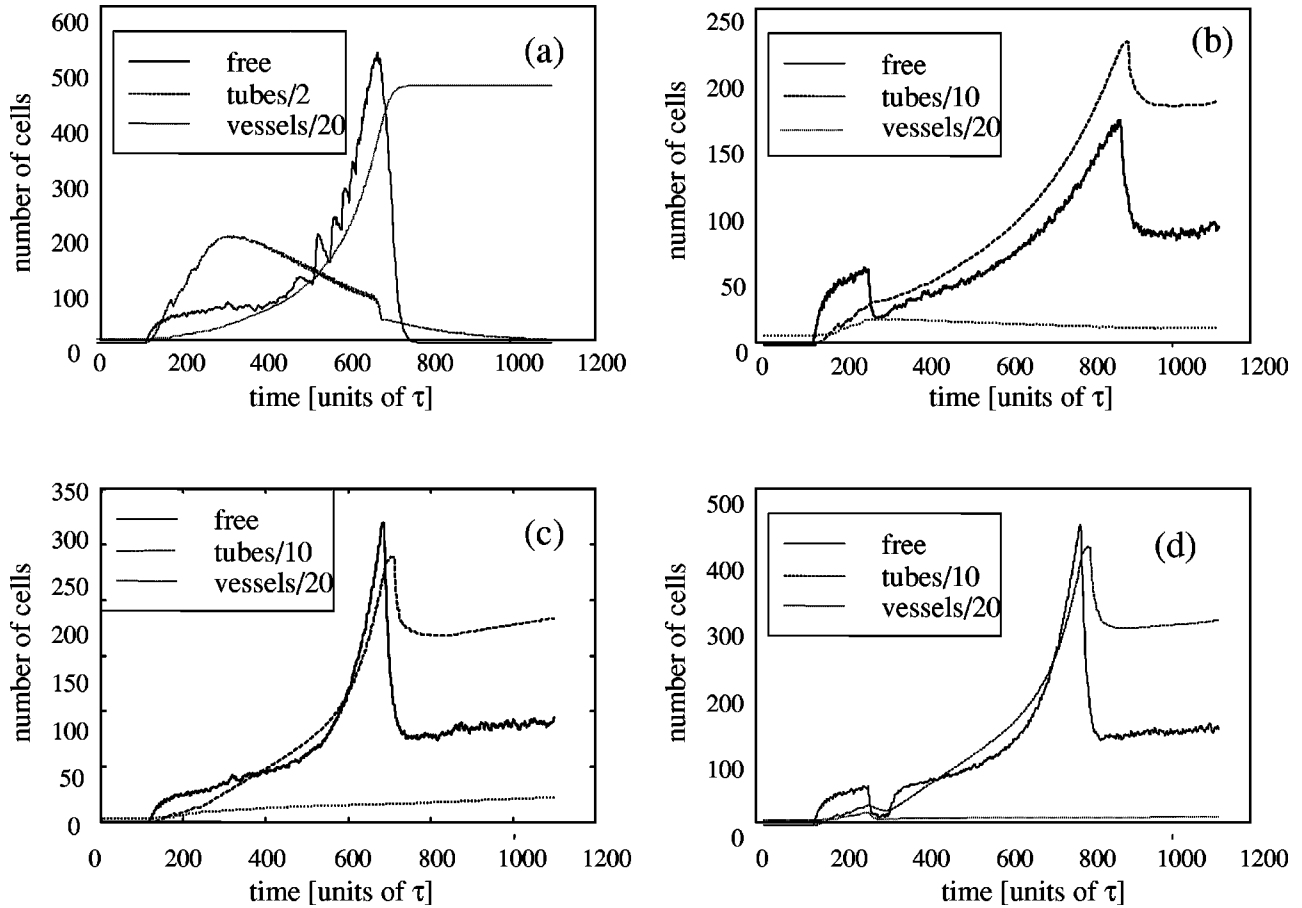
FIG. 2. Time evolution of the total number of the three endothelial cell populations, $c(1)$ (diffusing ECs), $c(2)$ (tube-forming ECs), and $c(3)$ (vessel ECs), for the cases: (a) without therapy; (b) with therapy I; (c) with therapy II; and (d) with therapy IV. All therapies are applied starting from $T=250$. (Note the different scales in the y axes and the different normalizations for the four plots.)

III. RESULTS AND DISCUSSION

In this section, we will present a few numerical results showing the modality of action of the drugs mentioned in the previous section and also analyze the effects related to the administration time and the drug duration.

The geometry is that of Ref. [9], i.e., a square $N \times N$ specimen, discretized into identical elements. The initial capillaries form an inverted T. We consider periodic boundary conditions at the left and right edges, while the lower edge is the tumor boundary, i.e., the TAF source and a nutrient sink. The upper edge is a TAF sink and a nutrient reflector.

For the values of the model parameters, we have chosen $\beta_0 = 0.01$, $M = 0.5$, $\chi = 40$, and $k = 0.1$ for all species. Additionally, $\alpha_p = 0.2$, $\alpha_v = 0.25$, $\lambda(1) = 0.1$, $\lambda(2) = 0.9$, $\varkappa_v = 0$, $\zeta_1 = \zeta_2 = 0.005$, $\beta_1(1) = \beta_1(2) = 0.03$, $\Gamma_1 = \Gamma_2 = 0.04$, $Q_2 = 0.25$, $\Psi = 0.004$, $S(1) = 2$; wherever $c_3 \neq 0$, and $S(2) = 0.2$ while the TAF source is active. The TAF source is stopped when the nutrient available for the tumor becomes twice as much as its initial value.

A. Angiogenesis failure induced by a therapy

In Fig. 2, we analyze the temporal evolution of the total number of ECs $[\Sigma_{i,j} c_{ij}(l)]$ for the three species in the case without therapy [Fig. 2(a)] and with the therapeutical protocols I, II, and IV applied at $T_1 = 250$ with an infinite duration of the drug effect. (Note the different scales in the y axes and the different normalizations for the four plots.)

In the case without therapy [Fig. 2(a)], we observe the existence of distinct phases in which different mechanisms dominate. This may suggest optimal applications for different drugs targeting different stages in the evolution of ECs towards maturation into vessels. In a first phase, therapies targeting the transformation from tube to vessels seems to be very little effective. In fact, up to $t \sim 200$, very few vessels are generated. Note that there is no delay between the formation of free ECs and tubes, while the formation of new vessels is slightly delayed. In a second phase, the tubes number increases very rapidly and vessels concentration starts increasing. This region seems to be the more sensitive to the action of any kind of drug, since all processes in the development of angiogenesis are equally active. Later, for $t > 300$, the transformation of tubes into vessels seems to be a fast (cascade) process with consequent reduction in the number of $c(2)$. At the same time, the formation of a large number of free ECs is observed. During this phase, only drugs of type IV (with direct apoptotic action) are expected to be efficient, while drugs controlling the transformation itself
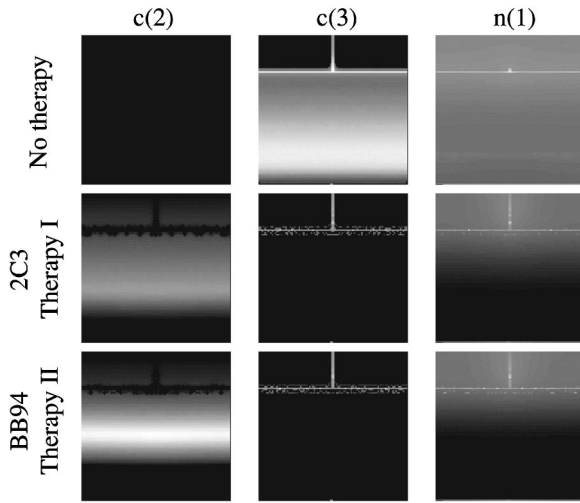
FIG. 3. Snapshots of the final distribution of tube-forming ECs $c(2)$, vessels $c(3)$, and nutrient $n(1)$ in the case without therapy and with therapies I and II applied at $T=250$. The original vessel distribution is visible as an inverted T in the central column.

FIG. 4. Snapshots at different times of the distribution of vessels $c(3)$ in the case without therapy and with two therapeutical protocols based on angiostatin ($T1=250$, $D1=50$; $T1=250$, $D1=20$ in the second and third rows, respectively).

may be completely ineffective due to the rapidity of the transformation processes. For $t>500$ the process rapidly reaches completion, the tumor, again well fed, stops emitting TAFs and the intermediate stage ECs, which have a finite lifetime, are rapidly reabsorbed. The number of vessels reaches a saturation value. The final configuration of the vessel distributions (reported in the Fig. 3) is in good qualitative agreement with experimental data [8,9].

In the three cases with therapy, the number of tubes and free ECs increase dramatically, while only a slight increase in the number of vessels is observed. A net of tubes, not connected with the vascular system, is formed close to the tumor front (see also Fig. 3), screening the diffusion of TAFs towards vessels and blocking the process. As expected, therapy I ($2C3$) causes a smaller proliferation of ECs due to the reduced absorption of TAFs [Fig. 2(b)] and consequent $c(1)$ reduction when the therapy is applied since proliferation does not compensate the $1 \rightarrow 2$ transformation any more. On the contrary therapy II [BB94-Fig. 2(c)] does not influence proliferation, but rather inhibits the transformation into vessels, with consequent increase in the number of $c(2)$. Free ECs does not proliferate as in the case without therapy since their principal source (cells belonging to vessels) is very reduced. Finally, the apoptotic effect on ECs is visible in Fig. 2(d), where an endostatin based therapy (therapy IV) is applied.

In Fig. 3, we report snapshots (lighter gray denotes higher densities) of the distribution of vessels $c(3)$, tubes $c(2)$, and nutrient $n(1)$ for the cases without therapy and with therapies I and II applied at the time $T_1=250$. When angiogenesis is successful, new capillaries grow from the original vessel distribution (inverted T) creating a large concentration of capillaries close to the tumor surface (located on the bottom part of the specimen). The nutrient available into the tissue grows very rapidly and TAF emission is stopped. As a consequence tubes and free ECs rapidly disappear.
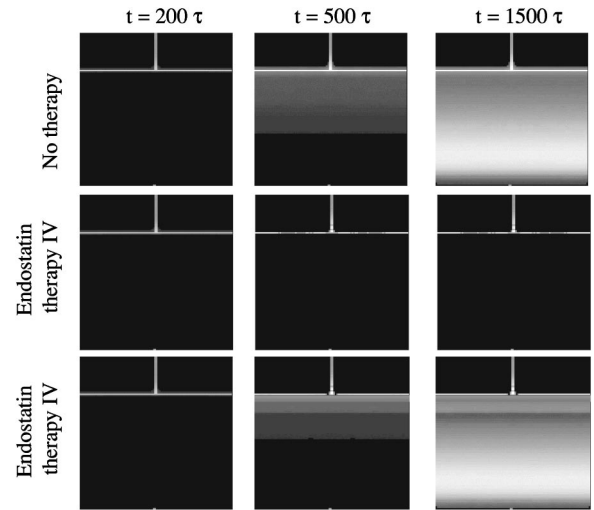
When therapies are applied, the angiogenetic process fails. In both cases only a few new capillaries are generated and are localized close to the original vessels, in agreement with experimental observations (see, e.g., Fig. 3 in Ref. [17]). Also, a depletion in the nutrient distribution may be observed due to the large consumption introduced by the presence of additional ECs $c(1)$ and $c(2)$, which cause an increase in the nutrient consumption. However, the process responsible for the failure of angiogenesis is rather different in the two cases. When therapy II is applied (e.g., a reduction in the remodeling capability), a large number of tubes are formed and screens completely the flux of TAF towards the original vessel, therefore stopping the angiogenetic process in the region between the tubes front and the original vessels. The connection between the new vascular structure formed by the $c(2)$ and the blood conveying vessels is inhibited. Tubes are more distributed in the case of therapy I. The screening effect is not so efficient and some angiogenetic activity is still present close to the original vessel, albeit very slow. It is expected that, in this second case, if the TAF source is not stopped (e.g., due to tumor starvation), at later times vessel connectivity between tubes and vessels may be reached and angiogenesis may take place [28].

Snapshots at different times of the evolution of the vessels distribution are reported in Fig. 4. The case without therapy is reported in the first row. The results with the application of endostatin (therapy IV) with two therapeutical protocols are also reported: $T_1=250$, $D_1=50$ (second row) and $T_1=250$, $D_1=20$ (third row). Only for large duration of the drug effect (second row) the therapy is effective, while, when the drug effect is very short in time, therapy results only in a delay of the process.

A different point of view is provided by Fig. 5, in which the total amount of nutrient $N(1)=\Sigma_j n_{i\,max,j}$ reaching the tumor is plotted as a function of time. When no therapy is applied, $N(1)$ increases monotonically with time up to when the formation of new vessels is stopped (about $t=650$).
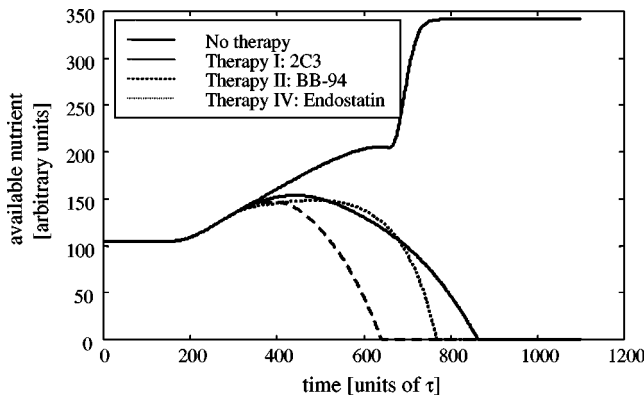
FIG. 5. Nutrient available for the tumor vs time in the cases with and without therapy as reported in the legend.

Then, a sudden increase is observed due to the disappearance of free and fixed ECs [see Fig. 2(a)], which were competing with the tumor in the nutrient acquisition. When any of the three therapies already discussed in Fig. 2 is applied, after an initial rise, $N(1)$ decreases abruptly. Under these conditions, the proliferation of nutrient-consuming endothelial cells in the intervening region would starve the tumor completely, since not supported by a conveniently growing vascular system.
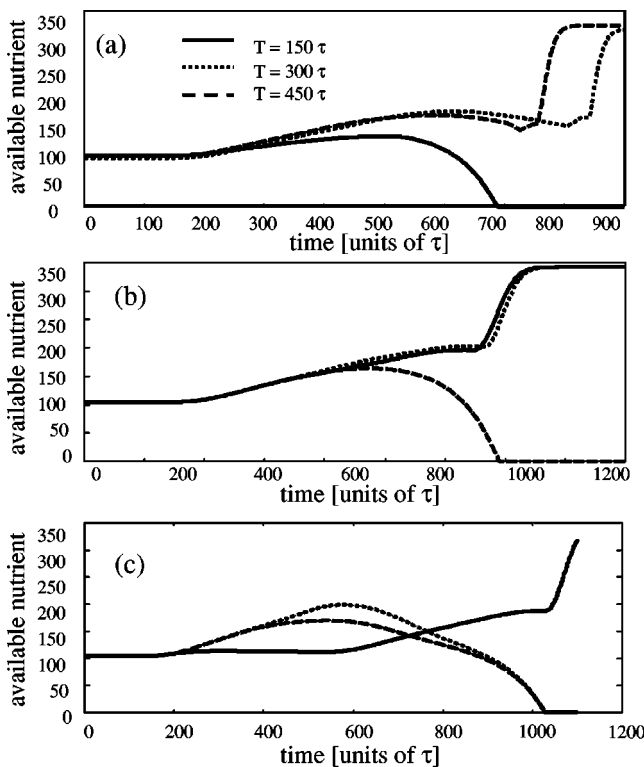
FIG. 6. Nutrient available for the tumor vs time for different times of application in the cases of therapy I (upper plot), therapy II (middle plot), and therapy IV (lower plot). Application times are reported in the figure. The duration of the drug effect is assumed to be $D1 = 100$ for all the cases considered.
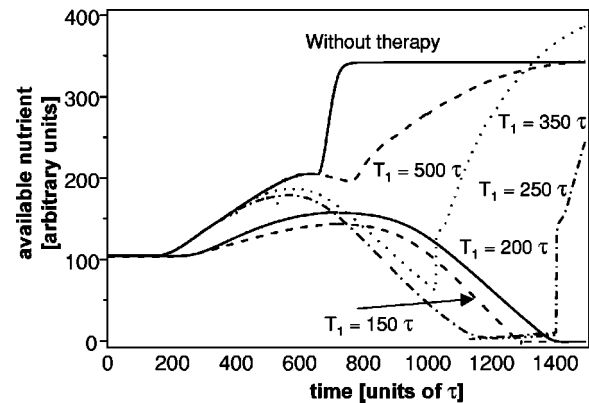
FIG. 7. Nutrient available for the tumor vs time for different administration times in the case of therapy I and infinite duration of the effect.

B. Effects of different therapeutical strategies

As already remarked, the therapy success is very sensitive to the adopted strategy. In Fig. 6, we analyze the effects of the three therapies discussed above when applied at different stages ($T_1 = 150, 300$, and 450) of the evolution of the system for a duration $D_1 = 100$. Therapy I (upper plot) is effective only if applied very shortly after the beginning of the angiogenetic process. Otherwise it will only result in a delay of the process or even (for $T_1 = 450$) have almost no effect at all (in the case without therapy the process was completed at about $t = 780$). Similar considerations apply for therapy II (middle plot). However, therapy II is successful only for intermediate values of T_1 and is completely ineffective if applied too early, due to the very reduced transformation rate from $c(2)$ to $c(3)$. Finally, as expected an endostatin-based treatment (lower plot) is ineffective if applied too early (due to the limited number of immature cells). The three therapies are all unsuccessfull if applied too late: in fact the cascade process cannot be controlled ($T_1 > 500$).

To further investigate the importance of the application time, in Fig. 7 we analyze the effects of therapy I applied at different instants, i.e., at different growth stages. Assuming an infinite duration of the effects, we notice that, as already remarked, therapy is succesful only when applied at suffi-
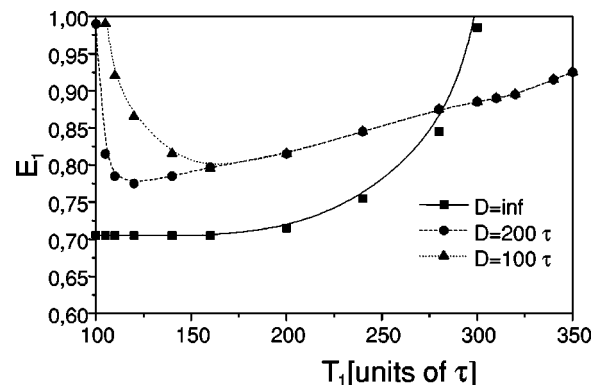
FIG. 8. Regions in the administration time-parameter variation space (T_1-E_1 space) in which therapy I is sucessful: infinite duration (solid line), $D_1 = 200$ (dashed line), and $D_1 = 100$ (dotted line).
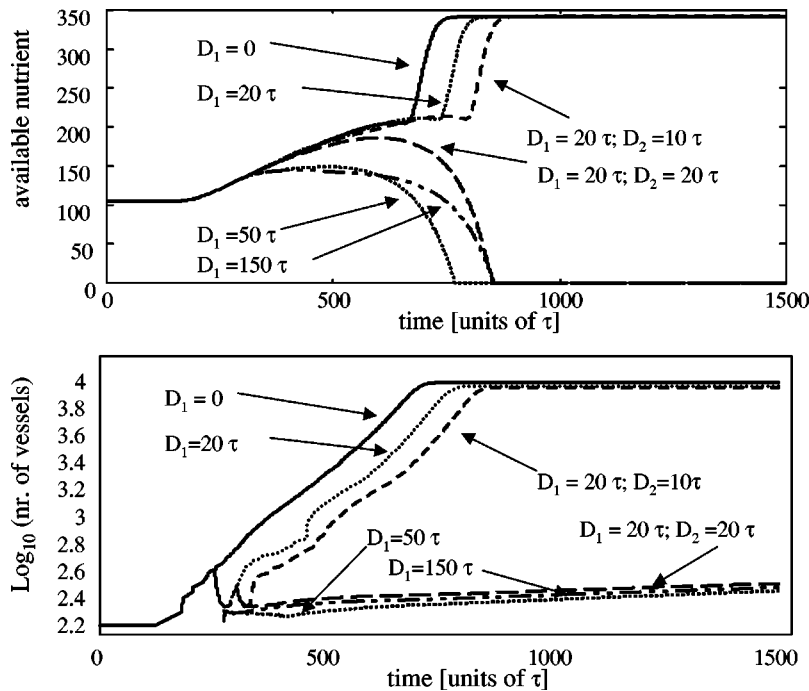
FIG. 9. Nutrient available for the tumor (upper plot) and logarithm of the number of vessels (lower plot) vs time for different therapeutical approaches based on endostatin.

ciently early stages ($T_1 = 150$ and 200). On the contrary, later treatment will only result in delaying the evolution of the angiogentic process.

In Fig. 8, we plot a phase diagram in the T_1-E_1 (time of administration-drug dose) space for therapies with different duration effects as reported in the legend. The behavior of the line separating the two phases (succesful and failed angiogenesis, below and above the curves, respectively) is not trivial. While it is expected that a drug acting permanently (infinite duration) becomes effective at lower doses when applied earlier (as displayed in the diagram), the behavior when the effect duration is finite looks very complex. The drug dose required to block angiogenesis is first decreasing than increasing with the application time, since early applications will have a limited effect since the process is just started. Also, it is expected that at intermediate times an infinite duration drug is more effective at lower doses. On the contrary, the behavior at large $T (T > 280)$ is counterintuitive, since short duration drugs seem to be more effective. However, the process can be explained by the fact that when the drug effect disappears and the TAF absorption coefficient is restored, $c(1)$ and $c(2)$ cells start reproducing again fastly and, if the front is sufficiently far from vessels (such is the case at late times during angiogenesis evolution), they may produce a screening effect, not developing when the proliferation rate remains slow (infinite duration).

Therapeutical success does not depend only on the application time but also on the drug duration effects. To analyze this dependence in the case of an endostatin-based therapy, we plot the available nutrient and number of vessels (in log scale) vs time in the upper and lower plots of Fig. 9, respectively, for different therapeutical strategies. In the cases of a single application of the drug at $T_1 = 250$, we observe that when the drug efficiency is very short in time ($D_1 = 20$) angiogenesis is still successful, albeit delayed with respect to the case without therapy ($D_1 = 0$). Increasing the duration of the effects ($D_1 = 50$ and $D_1 = 150$), the angiogenetic process is blocked. The same result can be obtained by repeating twice a short duration therapy ($T_1 = 250, D_1 = 20; T_2 = 350, D_2 = 20$). However, when the effects of the second application are shorter ($T_1 = 250, D_1 = 20; T_2 = 350, D_2 = 10$), the result is only an additional delay.

Finally, in Fig. 10 we consider the synergistic effects resulting from the simultaneous application of $2C3$ and BB94 (therapy III, infinite duration). The two therapies applied singularly are not effective. In fact, while a therapy based on BB94 causes a considerable delay, a $2C3$-based therapy is completely useless. However, when they are both applied, the angiogenetic process is not successful at all. Similar synergistic effects have been observed in several experimental trials (both *in vitro* and *in vivo*) and seems to pave the way for therapeutical approaches when saturation of the drug effect or toxicity for large doses are present.
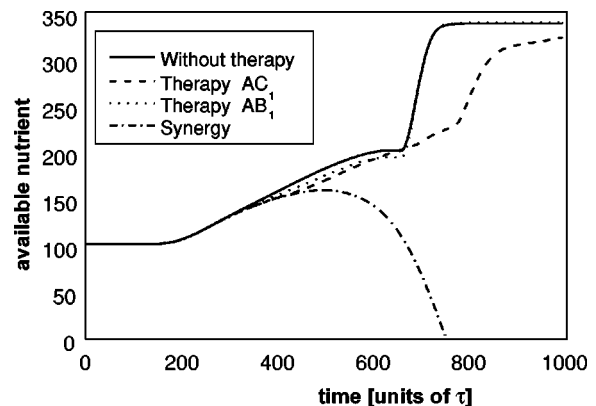
FIG. 10. Synergic action among therapies I and II. The temporal evolution of the nutrient available for the tumor is reported in the plot in the cases where no therapy is applied or when they are applied independently or simultaneously as reported in the legend.

IV. CONCLUSIONS

We have investigated how a simple "reaction-diffusion model" with evolving sources and sinks allows to simulate the progression of angiogenesis and its inhibition induced by the action of proper antiangiogenetic drugs. We have shown that therapies may be described in terms of a variation of the relevant parameters on which the drug acts. As a result, such variations may induce "phase transitions" from regions in the parameter space in which angiogenesis is succesful to regions in which it is inhibited.

We have analyzed in detail the effect of three therapeutical strategies, based on a TAF receptors inhibitor (the monoclonal antibody $2C3$ [26]), a remodeling inhibitor (the metalloproteinase inhibitor BB-94 [25]), and a drug creating an apoptotic signal for immature ECs (endostatin [23]). The results obtained through our simulations are in qualitative agreement with experimental data. The approach adopted in this paper has allowed us to study also the effects of different parameters in the therapeutical approach, such as the time of application and the duration of the drug effects. Also, synergic effects have been found between drugs targeting different stages in the angiogenetic process.

Although the approach presented here is very preliminary, it shows the possibility to apply physical concepts in the medical field. Even though qualitatively the results are independent of the model parameters, quantitatively an accurate estimate of the biological parameters used is necessary to make reliable predictions. Nevertheless, once the link between drug amounts and their effect on the cellular behavior at a microscopic level is established, models such as the one proposed here may become effective tools to test different strategies for the administration of the drug and eventually optimize them.

Finally, we remark that to compare with applications in "*in vivo*" growing tumors it is necessary to consider the interaction of the growing vascular system with a nonstationary source of TAFs [34]. However, preliminary results show that the considerations reported here still holds, at least qualitatively [35].

[1] G. Fáth and Z. Domanski, Phys. Rev. E **60**, 4604 (1999); S. Galam and J.P. Radomski, *ibid.* **63**, 051907 (2001).

[2] Z. Qu, J.N. Weiss, and A. Garfinkel, Phys. Rev. E **61**, 727 (2000).

[3] S.C. Ferreira, Jr., M.L. Martins, and M.J. Vilela, Physica A **261**, 569 (1998).

[4] M. Scalerandi, A. Romano, G.P. Pescarmona, P.P. Delsanto, and C.A. Condat, Phys. Rev. E **59**, 2206 (1999).

[5] A.R. Kansal, S. Torquato, G.R. Harsh, IV, E.A. Chiocca, and T.S. Deisboeck, J. Theor. Biol. **203**, 367 (2000).

[6] C.L. Stokes, D.A. Lauffenburger, and S.K. Williams, J. Cell. Sci. **99**, 419 (1991).

[7] M.J. Holmes and B.D. Sleeman, J. Theor. Biol. **202**, 95 (2000).

[8] B. Capogrosso Sansone, M. Scalerandi, and C.A. Condat, Phys. Rev. Lett. **87**, 128102 (2001).

[9] B. Capogrosso Sansone, C.A. Condat, and M. Scalerandi, Phys. Rev. E **65**, 011902 (2002).

[10] P.P. Delsanto, A. Romano, M. Scalerandi, and G.P. Pescarmona, Phys. Rev. E **62**, 2547 (2000).

[11] J. Folkman and M. Klagsbrun, Science **235**, 442 (1987); *Cancer Biology*, 2nd ed., edited by R. J. B. King (Pearson Education, Harlow, England, 2000).

[12] M.F. Carlevaro *et al.*, J. Cell Biol. **136**, 1375 (1997).

[13] D. Hanahan and J. Folkman, Cell **86**, 353 (1996).

[14] W. Risau, Nature (London) **386**, 671 (1997).

[15] J. Folkman, *Cancer Medicine*, edited by J. F. Holland *et al.* (Decker, Ontario, 2000), pp. 132–152.

[16] M.I. Koukourakis *et al.*, Cancer Res. **60**, 3088 (2000).

[17] J.M. Wood *et al.*, Cancer Res. **60**, 2178 (2000).

[18] R.S. Kerbel, Nature (London) **390**, 335 (1997).

[19] T. Boehm, J. Folkman, T. Browder, and M.S. O'Reilly, Nature (London) **390**, 404 (1997).

[20] H.J. Mauceri *et al.*, Nature (London) **394**, 287 (1998).

[21] W. Arap, R. Pasqualini, and E. Ruoslahti, Science **279**, 377 (1998).

[22] R. Cao *et al.*, Proc. Natl. Acad. Sci. U.S.A. **96**, 5728 (1999).

[23] P. Blezinger *et al.*, Nat. Biotechnol. **17**, 343 (1999).

[24] M. Dhanabal *et al.*, J. Biol. Chem. **274**, 11721 (1999).

[25] G. Bergers, K. Javaherian, K.-M. Lo, J. Folkman, and D. Hanahan, Science **284**, 808 (1999).

[26] R.A. Brekken, J.P. Overholser, V.A. Stastny, J. Waltenberger, J.D. Minna, and P.E. Thorpe, Cancer Res. **60**, 5117 (2000).

[27] P. Carmeliet and R.K. Jain, Nature (London) **407**, 249 (2000).

[28] B. Capogrosso Sansone, C. A. Condat, F. Peggion, and M. Scalerandi (unpublished).

[29] H.A. Levine *et al.*, Bull. Math. Biol. **63**, 801 (2001).

[30] P.P. Delsanto *et al.*, Wave Motion **16**, 65 (1992); G. Kaniadakis, P.P. Delsanto, and C.A. Condat, Math. Comput. Modell. **17**, 31 (1993).

[31] J.C.M. Mombach and J. Glazier, Phys. Rev. Lett. **76**, 3032 (1996).

[32] T. Hofer, J.A. Sherratt, and P.K. Maini, Physica D **85**, 425 (1995).

[33] C.A. Condat and G.J. Sibona, Recent Res. Dev. Stat. Phys. **1**, 61 (2000); H. Taitelbaum and Z. Koza, Physica A **285**, 166 (2000).

[34] M. Scalerandi and B. Capogrosso Sansone (unpublished).

[35] M. Scalerandi, M. A. Garella, and B. Capogrosso Sansone (unpublished).